Available online at www.sciencedirect.com

ScienceDirect

Energy Procedia 00 (2018) 000–000

Energy Procedia

www.elsevier.com/locate/procedia

73rd Conference of the Italian Thermal Machines Engineering Association (ATI 2018), 12–14 September 2018, Pisa, Italy

Exergy Analysis of a PWR Nuclear Steam Supply System - II part: a case study

Luisa Ferroni[1] *, Antonio Natale[1]

Affiliation[1]; DIAEE, Sapienza Università di Roma, Italy

Abstract

The paper shows the results of the exergetic analysis of the Nuclear Steam Supply System (NSSS) of the MARS Pressurized Light Water Reactor using the theoretical methodology described in the authors' previous works [1] and [2]. The analysis firstly aims at a novel assessment of the irreversibilities occurred in the nuclear reactor vessel to compare the results, in terms of Exergy Destruction and exergetic Efficiency, with those obtained adopting one of the most employed methodology as reference.

The comparison showed that a detailed exergetic analysis, mainly aimed to strictly assess the fission temperature, can lead to a higher estimate of the PWR exergetic Efficiency values.

Keywords: Exergy analysis; Energy conversion; Thermodynamic simulations; Pressurized Water Reactor; Fission energy.

* Corresponding author. Tel.: 0039 06 49918648
E-mail address: luisa.ferroni@uniroma1.it

1. Introduction

The methodology described in Part I of this paper [2] has been applied to the MARS (Multipurpose Advanced Reactor inherently Safe) PWR reactor [3, 4]. The most important aim of the work is the comparison between the values of exergetic Efficiency of the nuclear reactor obtained by the authors applying the new methodology proposed in [1] and [2] with those obtained applying, at the same reference plant, the most established methodology adopted by other authors. In the last methodology, the Fission Exergy is assumed to be equal to the Fission Thermal Power, that is to assume the Carnot Factor equal to one and, consequently, to hypothesise an extremely high fission temperature.

Nomenclature

c_p	isobaric specific heat, J kg^{-1} K^{-1}	E_f	fission Energy, J
ex	specific Exergy, kJ kg^{-1}	ex_i	specific flow Exergy, kJ kg^{-1}
$\dot{E}x$	total Exergy, MW	$\dot{E}x_\delta$	total Exergy destruction, MW
$\dot{E}x_q$	heat transfer Exergy, MW	F_P^A	axial peak factor
g	gravity acceleration, m s^{-2}	h	specific enthalpy, kJ kg^{-1}
h_{wall}	convection coefficient, W m^{-2} K^{-1}	H_a	fuel rod active length, cm
H_e	fuel rod extrapolated length, cm	K	thermal conductivity, W m^{-1} K^{-1}
K_a	adduction coefficient, W m^{-1} K^{-1}	K_{He}	gap (Helium) thermal conductivity, W m^{-1} K^{-1}
K_{UO2}	fuel (uranium dioxide) thermal conductivity, W m^{-1} K^{-1}	K_{Zirc}	cladding(Zircaloy) thermal conductivity, W m^{-1} K^{-1}
$\dot{L}$	Work flow, kW	$\dot{m}$	mass flow rate, kg s^{-1}
$\dot{m}_{BOP}$	Balance of Plant (SG secondary side) mass flow rate, kg s^{-1}	$\dot{m}_{RCS}$	Reactor Coolant System mass flow rate, kg s^{-1}
$\dot{m}_{SC}$	sub-channel coolant mass flow rate, kg s^{-1}	M	molecular weight, g mole^{-1}
N_A	Avogadro's number	$N_{fr,i}$	Number of fuel rods with "i" enrichment level
p	pressure, bar [Pa]	P_{el}	Reactor Coolant Pump electric power, MW
q'	linear power density, Wcm^{-1}	$\bar{q}'$	average linear power density, Wcm^{-1}
$\bar{q}'''$	average volumetric power density, Wcm^{-3}	$\dot{Q}$	heat transfer rate, kW_{th}
r	generic radius, cm	R_{ext}	External radius, cm
RF	Robertson Factor	R_g	gap (Helium) radius, cm
R_p	fuel pellet (uranium dioxide) radius, cm	s	specific entropy, kJ kg^{-1}K^{-1}
S_g	fuel rod gap thickness, m	$\dot{S}$	total entropy, kW K^{-1}
S_c	clad thickness, mm	$\dot{S}_{gen}$	total entropy generation, kW K^{-1}
T	temperature, K	$T_{A,P}$	average SG primary side temperature, K
$T_{A,S}$	average SG secondary side temperature, K	T_{avf}	average fuel pellet temperature, K
Tb	bulk(coolant) temperature, K	Tc	central fuel rod temperature, K
$T_{ext,SG}$	external SG surface temperature, K	T_{He}	gap (Helium) temperature, K
T_{ig}	internal cladding temperature, K	T_{fiss}	fission temperature, K
T_S	surface pellet temperature, K	T_{vessel}	average vessel temperature, K
T_w	wall (cladding) temperature, K	V	volume, cm^3
w	velocity, m s^{-1}	X_i	generic fuel enrichment level (percentage)
z	height, cm		

Subscript

0	reference state of environment	b	bulk/coolant (water)
c	central axis of fuel rod	F	fuel
fiss	fission	gen	generated
ig	cladding internal side (zircaloy)	H/CLV	Hot/Cold dummy valve
hyp	hypotetical	in	inlet
Loss	transferred to the environment	MAX	maximun
out	Outlet	P	Product
q	Related to heat transfer	r	real
RCP	Reactor Coolant Pump	RPV	Reactor Pressure Vessel
S	pellet surface	SG	Steam Generator
th	thermal	UO_2	Uranium oxide
w	Wall (cladding surface)		

Greek Symbols

δ	adjunctive lenght, cm	ε_{UO2}	fuel (uranium dioxide) emissivity
ε_{Zirc}	cladding (Zircaloy-4) emissivity	η_{Ex}	exergetic efficiency (2nd law efficiency)
$\bar{\Phi}_n$	average neutronic flux, neutrons cm^{-2} s^{-1}	ρ_{UO2}	fuel (uranium dioxide) density, g cm^{-3}
σ	Stefan – Boltzmann constant, W m^{-2} K^{-4}	σ_f	microscopic fission cross section (UO_2), barn (cm^2)
σ_{tot}	total microscopic cross section (H_2O), barn (cm^2)	Σ_{tr}	macroscopic transport cross section (H2O), cm^{-1}

2. Case Study - Determination of Exergetic Efficiency for MARS Reactor Coolant System

2.1 MARS NPP description

The MARS Reactor [3, 4] is a Pressurized Water Reactor included in the SMR new generation fleet (the International Atomic Energy Agency defines “Small” the nuclear reactors as under 300 MWe), characterized by compact factory-fabricated design, high reliability, greenhouse gases emission free. MARS NPP was designed to produce electric energy and/or thermal energy useful for a wide range of applications, for example desalination and district heating. The MARS core cooling system includes only one loop, equipped with one vertical-axis U-tube Steam Generator and one canned rotor pump directly connected to the Steam Generator outlet nozzle as depicted in figure 1. The MARS primary loop incorporates several innovative features that hugely improve the safety performances, in particular the presence of a secondary pressurized containment, filled with warm water (70°C reference temperature), enveloping all RCS components, except for the SG, with the aim to avoid any loss of primary coolant (LOCA, Loss of Coolant Accident). The MARS reactor main technical characteristics are listed in Table 1; data referring to the other main RCS components are listed in Table 2. Data refer mainly to the last published version of MARS report [3], with some updates based on subsequent design developments.

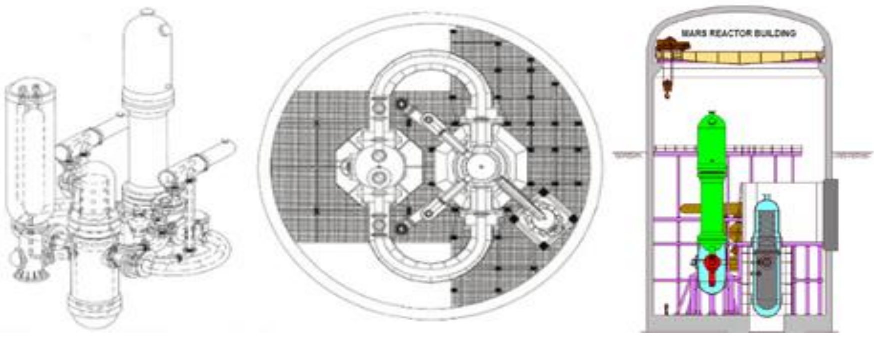

Figure 1. MARS primary loop (enveloped in the Containment Primary Protection) and reactor building section [3, 4]

2.2 Exergy analysis of MARS RPV

To perform the Exergy analysis of the MARS RPV on the base of the new methodology described in [1] and [2], referring to a real operational condition, the following simulation data and hypotheses have been taken into account:

- first steady state of reactor in first operation;
- average energy released for each fission equal to 200 MeV (excluded neutrinos’ Energy);
- reference conditions of the environment for exergy assessment:

P_0=101.3 kPa; T_0=298.15 K; s_0=0.367 kJ/kg K; h_0=104.93 kJ/kg [5].

Referring to the modeling described in [1] and [2], theoretical and numerical updates have been performed:

- the actual MARS core design, reported in Table1, which prescribes three enrichment levels of fuel assemblies, has been implemented. Consequently, coolant flow is not radially constant but it is proportionally higher in the sub-channels characterized by more elevated enrichment levels of fuel rods.
- to assess heat exchange between cooling water and pellet central temperature, the Fourier equation has been adopted and the following updates, in terms of heat exchange coefficients, have been carried out:
  - ✓ for heat transfer in the clad, Zircaloy conductivity has not been considered independent from temperature, but the following equation [6] has been introduced to get T_{ig} :

$$K_{Zirc}(T) = 12.767 - 5.4348\times10^{-4}\,T + 8.9818\times10^{-6}\,T^2 \quad \text{[W/m K]} \qquad (1)$$

Table 1. MARS Reactor main characteristic data

Reactor Type	Thermal Reactor	PWR
Thermal Power Fission generated in the Core	625.2	MWth
Reactor Coolant Inlet/Outlet Temperature	214/254	°C
Reactor Coolant Flow Rate trough the Core	3227	Kg/s
Reactor Coolant System (RCS) Flow rate (forced flow)	3337.44	Kg/s
Reactor Average Neutronic Flux	1.978×10^{13}	Neutr/cm^{2}s
Fission Cross Section U235	577	barn
Operating Pressure (Core Outlet)	75	bar
Average Operating Temperature (Coolant)	235	°C
Fuel Pellet Material	Sinterized UO_2	(95%D.T.)
Fuel Pellet Density	10.421	g/cm^3
Fuel volume for each rod	131.933	cm^3
Fuel Rod Array	17 x 17	
Fuel Rods per Fuel Assembly (active channels)	264	
Fuel Bundles (Assemblies)	89	
Fuel Rod Percentage Enrichment (X_1, X_2,X_3)	X_1 = 1.9% (33 Assemblies) X_2 = 2.3% (28 Assemblies) X_3 = 3.0% (28 Assemblies)	
Fuel Rod External Diameter	0.95	cm
Fuel Rod Active Lenght	260	cm
Fuel Rod Gap Thickness (Helium)	100×10^{-6}	m
Fuel Rod Cladding Thickness (Zircaloy-4)	0.63	mm
Fuel Rod Pitch	1.26	cm
Fuel Rod Pitch to Diameter Ratio (square lattice)	1.32	//
Fuel Rod Average Linear Power Density (X_2)	99.234	W/cm
Fuel Rod Average Volumetric Power Density (X_2)	195.565	W/cm^3
Control Rod Guide Tube Diameter	1.224	cm
Core Average Volumetric Power Density (X_2)	56.5	kW/l
Axial Peak Factor	1.565	//
Core Pressure Drop	31	kPa
Containment Coolant Primary Water Temperature	70	°C
Vessel		
-Internal Diameter/Thickness	300\12	cm
-Cylinder Height	805.6	cm
-Upper / Lower head thickness	8	cm
-Upper / Lower head internal radius	141\150	cm
- Material	Carbon Steel (SA533Gr.BCl.1)	

Table 2. MARS Reactor Steam Generator and Primary Coolant Pump characteristic data

STEAM GENERATOR		
Steam flow rate outlet	277.6	Kg/s
Steam pressure outlet	18.8	bar
Steam temperature outlet	209.3	°C
Steam moisture outlet	0.25	%
Feedwater inlet temperature	151.2	°C
Feedwater inlet pressure	21.8	bar
PRIMARY REACTOR COOLANT PUMP		
Total efficiency	0.874	
Total head	5.72	bar

- ✓ To assess heat transfer in the internal gap of the clad, a temperature trend has been simulated taking into account, apart from helium thermal conductivity (helium is stagnant), a heat transfer supplement due to thermal radiation between internal clad surface, T_{ig}, and external pellet surface, T_s, using the following relationships [1, 7] :

$$T_S = T_{ig} + \frac{q' \ln\langle {}^{Rg}/_{R_P}\left(1+{}^{Sg}/_{R_P}\right)\rangle}{2\pi K_a} \tag{2}$$

$$K_a = K_{He} + \frac{s_g \sigma \langle T_S^4 - T_{ig}^4\rangle}{\langle \frac{1}{\varepsilon_{UO2}} + \frac{1}{\varepsilon_{Zirc}} - 1\rangle\langle T_S - T_{ig}\rangle} \tag{3}$$

- ✓ the emissivities being assessed as follow [6,8]:

$$\varepsilon_{UO2}(T_s) = 0.7856 + 1.5263\times10^{-5}\, T_s \tag{4}$$

$\varepsilon_{Zirc} = 0.80846$ (Zircaloy oxide thickness has been assumed equal to zero) (5)

- ✓ The equation to assess fuel centerline temperature has been corrected multiplying the second term by the Robertson Factor, RF, to take into account the mean value of heat distribution in the fuel pellet depending on the enrichment level, X, and on pellet radius Rp [7] :

$$q'(z) = 4\pi\ RF\int_{Ts}^{Tc} K_{UO2}(T)\, dT \qquad (-H_a/2 \le z \le +H_a/2) \tag{6}$$

- ✓ In the present work RF (X, Rp) has been assumed as constant and equal to 0.97 because Rp is constant and the dependence on reference enrichments is negligible [7].
- ✓ Cooling water cp has been considered variable as a function of temperature. To assess cp trend a linear interpolation (integration step,1 K) between cooling water inlet/outlet core temperature cp was adopted [5].
- ✓ In the core, a cooling water bypass factor of 3% has been considered.

- To obtain the extrapolated fuel rod height He, the adjunctive length δ, necessary to obtain the correct position of the zero neutronic flux boundary condition has been calculated as in [1] but Σtr, the macroscopic transport cross section, has been obtained by means of actual σ_{tot} values from [9,10].
- Vessel temperature has been calculated in detail taking into account the actual temperature values inside and outside the vessel, applying thermal conduction and thermal convection laws for the specific materials and fluids.
- To assess temperatures profiles, Fourier's equation has been applied using step of 1 cm (the pellets height).

By applying the above updates to the modeling approach reported in [1] and [2], all temperature profiles, $T_b(z)$, $T_w(z)$, $T_{ig}(z)$, $T_{He}(z)$, $T_S(z)$, and $T_c(z)$, were calculated for the three reference MARS enrichments, using an integration of Fourier's equation (step of 1 cm) as shown in Figure 3(a). Best fit interpolation curves were evaluated to join, for each enrichment level, the 261 T_c and T_s temperatures values. In Figure 3(b) the 2.3% enrichment curves are shown.

$T_{fiss}(z)$ has been evaluated, for each enrichment level, as the average value of $T_c(z)$ and $T_s(z)$, having assumed $T_{fiss,i}(z) = T_{avf,i}(z)$. Once the $T_{fiss,i}(z)$ pattern has been known using equations (9b), (13) and (14) shown in [2], the total fission thermal power Exergy has been calculated for the actual core:

$$\dot{E}x_{Qfiss(r)} = \dot{E}x_{Fuel} = 449.51\ MW_{th}$$

Therefore, Total Exergy Product has been computed using equation (15) shown in [2]:

$$\dot{E}x_{Product} = 257.16\ MW_{th}$$

Knowing $\dot{Q}_{Loss,RPV}$ by Energy balance, thermal power loss has been computed using eq. (16) shown in [2], and using data from Table 3:

$$\dot{Q}_{Loss,RPV} = 0.465\ MW_{th}$$

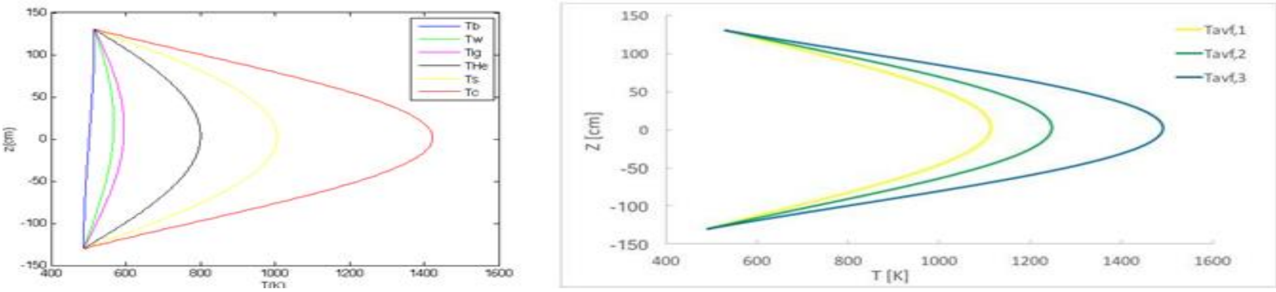

(a) (b)

Figure 2. Actual temperature profiles for X = 2.3% (a) and average temperature profiles of the core $T_{avf,i}(z)$ (b)

Total RPV Exergy Loss has been computed as assessed in equation (17) shown in [2] ,just knowing the average vessel temperature. To determine $\dot{E}x_{Loss,RPV}$, the average vessel temperature determination must be calculated by assessing internal and external vessel temperatures. For the evaluation of the vessel internal temperature Dirker–Meyer correlation for annular forced flows [11] has been chosen; to determine vessel external temperature, taking into account vessel conductivity [12], Fourier's equation has been adopted:

$$\dot{E}x_{Loss,RPV} = 0.17\ MW_{th}$$

Exergy Destruction RPV has been calculated using equation (7) shown in [2]:

$$\dot{E}x_{\delta,RPV(r)} = 192.18\ MW_{th}$$

consequently, MARS RPV Exergetic efficiency, assessed as in equation (8) shown in [2], has been computed:

$$\eta_{Ex,RPV(r)} = 1 - \frac{0.17+192.18}{449.51} = 57.21\%$$

On the base of some of the above results obtained for the effective MARS operational conditions, it has been possible to perform the Exergetic analysis in the hypothetical reference condition described in chapter 1, that is $T_{fiss} >> T_0$ [13, 14, 15 et al.]. In accordance with this working hypothesis, the total Fission Exergy value is:

$$\dot{E}x_{Qfiss(hyp)} = \dot{E}x_{Fuel} = \dot{Q}_{fiss} = 625.2\ MW_{th}$$

Knowing Total Exergy Product and Total RPV Exergy Loss as above calculated, using Equation (7) shown in [2], the RPV Total Exergy Destruction can be assessed:

$$\dot{E}x_{\delta,RPV(hyp)} = 367.87\ MW_{th}$$

Finally, MARS RPV Exergetic efficiency, according to equation (8) shown in [2], can be computed as follow:

$$\eta_{Ex,RPV(hyp)} = 1 - \frac{0.17+367.87}{625.2} = 41.13\%$$

2.3 Exergy analysis of MARS Reactor Coolant System, RCS

Referring to the scheme depicted in Figure 5 in [2], all RCS components are assumed as adiabatic components (except RPV and SG) and a steady state operational mode is considered. Knowing mass flow rates, pressures and temperatures from Tables 1 and 2, specific and total Exergy flow rates were calculated [5] using equation (18) shown in [2]. The results are listed in Table 3.

As regards the Steam Generator, whose P.P.S. in shown in Table 1 in [2], knowing steam and water flow rates and input and output specific Energies and Exergies (see Table 3), Exergy Fuel and Exergy Product and Exergy Loss have been assessed using the following equations:

$$\dot{Q}_{Loss,SG} = \dot{m}_{RCS}(h_3 - h_4) - \dot{m}_{BOP}(h_7 - h_6) \quad (7)$$

$$\dot{E}x_{Loss,SG} = \dot{Q}_{Loss,SG}\left(1 - \frac{T_0}{T_{ext,SG}}\right) \quad (8)$$

Table 3. Thermodynamic data and specific and total Exergies of RCS nodes [5]

	m [Kg/s]	P [bar]	T [K]	h [kJ/kg]	s [kJ/kgK]	x [dim.less]	ex [kJ/kg]	Ex [MW]
Flow 1 (Water)	3337.44	75.87	487.15	917.83	2.45	0.00	191.12	637.85
Flow 2 (Water)	3337.44	74.67	527.15	1105.02	2.82	0.00	268.17	895.01
Flow 3 (Water)	3337.44	73.30	527.15	1105.02	2.82	0.00	268.07	894.67
Flow 4 (Water)	3337.44	71.43	487.15	917.68	2.45	0.00	190.74	636.59
Flow 5 (Water)	3337.44	77.15	487.26	918.39	2.45	0.00	191.43	638.89
Flow 6 (Water)	277.60	21.80	424.35	638.47	1.85	0.00	90.71	25.18
Flow 7 (Water)	277.60	18.80	482.45	2792.32	6.35	0.9975	902.94	250.66
Flow 8 (Electric Power)	-	-	-	-	-	-	-	2.73
Flow 9 (Thermal Power)	-	-	-	-	-	-	-	449.51

To achieve SG Exergy Loss, external surface temperature has been assessed using the following equation [16]:

$$T_{ext,SG} = \frac{T_{A,P}+T_{A,S}}{2} = \frac{{(T_3+T_4)}/{2} + {(T_6+T_7)}/{2}}{2} \quad (9)$$

The Reactor Coolant Pump, RCP, has been assumed as an adiabatic component. Referring to its P.P.S. reported in Table 1 in [2], and using the technical values reported in Table 2 and Table 3, is possible to assess its Exergy Destruction and exergetic Efficiency. Finally, Exergy Destructions and exergetic Efficiencies of all main RCS components have been assessed using equations (5) and (6) shown in [2].

2.4 Results and discussion

Final results and comparisons between real case and are shown in Table 4 and depicted in Figures 3 and 4.

Table 4. Exergy Destructions and Exergetic Efficiencies of MARS RCS main components

	Physical Productive Structure			Exergy Analysis RCS MARS NPP	
	Ex.Fuel [MW_{th}]	**Ex.Product[MW_{th}]**	**Ex.Loss [MW_{th}]**	**Exergy Destruction [MW_{th}]**	**η_{ex}[%]**
RPV (hyp)	*625.2*	*257.16*	*0.17*	*367.87*	*41.13%*
RPV (real)	*449.51*	*257.16*	*0.17*	*192.18*	*57.21%*
SG	258.08	225.47	10.36	22.25	87.36%
RCP	2.71	2.30	0.00	0.41	84.87%

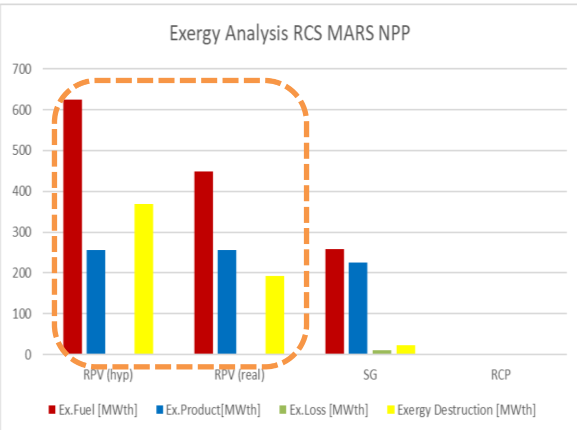

Figure 3. Exergy Fuel, Product, Loss and Destruction of MARS main RCS components

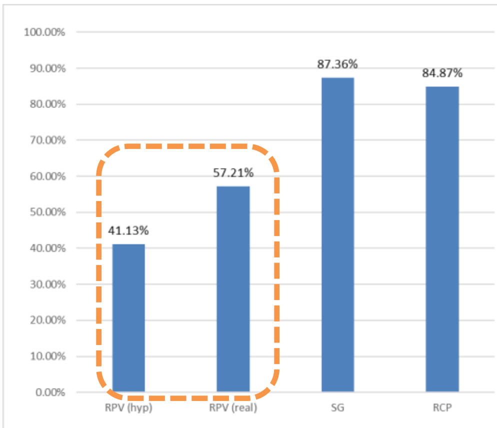

Figure 4. Exergetic Efficiences of MARS main RCS Components

The most important result of the paper is the comparison between the value of Exergy Destruction and exergetic Efficiency of the nuclear reactor as assessed in the new methodology proposed, with those obtained applying the reference methodology. With reference to the destroyed Exergy, the highest value obtained with the reference comparison methodology is due to the fact that the fission temperature is hypothesized to be extremely high (the Carnot Factor would assume unit value), certainly much higher than the actual one in a real reactor (using the new methodology, MARS reactor' T_{fiss} is variable between 500 up to 1500 ° K). In support of the above, it is important to underline that, for reasons of nuclear safety and technological constrains, the maximum fission temperature must be tightly controlled so that it does not exceed just about 1.500 K in order to avoid potential core melting accidents.

Furthermore, the lower temperature which fission thermal energy is available in an actual reactor justifies the reduced fission Exergy, because energy, available at lower temperature, has a lower availability to provide work.

On the basis of these considerations, for the same Exergy Product of RPV, is also justified the higher value of the exergetic Efficiency referred to the real case, and this implies that the exergetic content of the nuclear fuel seems to be better exploited than expected by the methodology in reference [13, 14, 15].

Finally, it could be interesting to note that the value of the RPV exergetic efficiency assessed by the authors for the MARS Reactor is comparable with the exergetic efficiency of a fossil-fuelled combustion chamber (e.g. 56% as assessed in [17]). As also the P.P.S.s are almost the same, these considerations could allow to draw a parallelism between a Nuclear Reactor and a conventional combustion chamber at least in terms of exergetic efficiency.

3 Conclusions

The first aim of the previous works [1,2] has been to perform an exergetic analysis of a nuclear Pressurized Water Reactor in which all heat exchange phenomena in the reactor core are assessed in detail. The results shown in this paper, a test case that includes the thermodynamic behavior of all main components of the MARS Nuclear Steam Supply System (NSSS), allow to compare the numerical results of the proposed methodology with those of other similar research in which simplifying work hypotheses about fission temperature were adopted. These results seem to demonstrate that a more detailed simulation of all heat transfer phenomena in the PWR nuclear reactor, in particular a strictest definition of the fission temperature, allow to get higher exergetic Efficiency of the nuclear reactor itself.

References

[1] Ferroni, L., Natale, A., and Gatto, R..”Exergy Analysis of a PWR Core Heat Transfer”. *Int. Journal of Heat and Technology, Vol. 34 Special Issue 2 (2016), pp. S465-S471. DOI:* https://doi.org/10.18280/ijht.34S239

[2] Ferroni L., Natale A., “Exergy Analysis of PWR Nuclear Steam Supply System-Part I”, Energy Procedia *00,(2018).*

[3] DINCE, University of Rome. “600 MWth MARS Design Progress Report”, *3rd ed., Rome, Italy ,(2003).*

[4] ENEA, Dipartimento Energia, Settore Energia Nucleare da Fissione. “MARS Multipurpose Advanced Reactor inherently Safe - Rapporto di Valutazione di Sicurezza”, *Bologna, Italy,(1994)*.

[5] *International Steam Tables – IAPWS - IF97 available on website: www.thermodynamics-zittau.de.*

[6] IAEA, *“Thermophysical properties database of materials for Light Water Reactors and H.W. reactors: Final report of a coordinated research project 1999–2005”, IAEA-TECDOC1496; Vienna, Austria (2006); p.50; p. 249.*

[7] Cumo M., *“Impianti Nucleari”, 1st ed. Ed. La Sapienza, Rome, Italy, 2008; pp.472-478; 512-525; 526-528; 618-620.*

[8] Idaho National Laboratory (INL). *“NUREG/CR-6150-Rev.2”, Vol.4(PT3); Idaho Falls, ID 83415-3129, (2001); pp. 5-16 (available on website* https://www.nrc.gov/docs/ML0103/ML010330422.pdf*).*

[9] Dritsa, M., and Kostikas, A. *”Total cross section of water at room temperature and 200 DEG C. (1967)”, Data retrived from the EXFOR database version of February 01, 2017 and available on website* http://www-nds.iaea.org/EXFOR/20176.001.

[10] Marquez Damian, J.I., Granada, J.R., and Malaspina, D.C. *“New thermal neutron scattering kernels for light and heavy water based on molecular dynamics simulations”. Physics Procedia (2014), Vol. 60, pp.300 – 309.*

[11] Dirker,J., and Meyer,J.P. *“Convective heat transfer coefficients in concentric annuli”. Energy Heat transfer engineering (2005), Vol. 26 Issue 2, pp. 38-44. DOI: 10.1080/01457630590897097*

[12] ASM International Metals Handbook. *”Properties and Selection: Irons, Steels, and High performance alloys”, Vol.1. 10th Ed. (1990).*

[13] Durmayaz, A. and Yavuz, H.. *“Exergy analysis of a pressurized-water reactor nuclear-power plant”. Applied Energy (2001) ,69, pp 39-57.*

[14] Sayyaadi, H. and Sabzaligol T.. *“Various approaches in optimization of a typical pressurized water reactor power plant”. Applied Energy (2009), 86, pp 1301-1310.*

[15] Terzi, R., Tukenmez, I., and Kurt, E.. *“Energy and Exergy analyses of a VVER type nuclear-power plant”. Int. Journal of Hydrogen Energy (2016), Vol 41, Issue 29, pp 12465-12476.*

[16] Molinari, G. *“Massa ed energia nella combustione tecnica”, Ed. Aracne: Rome, Italy (2013) pp. 409-416.*

[17] Borel, L., and Favrat, D. *“Thermodynamics and Energy systems analysis”. EFPL Press Ed. (2010) p. 584-585.*